Available online at www.sciencedirect.com
SCIENCE DIRECT®
International Journal of Machine Tools & Manufacture 44 (2004) 595–605
INTERNATIONAL JOURNAL OF MACHINE TOOLS & MANUFACTURE DESIGN, RESEARCH AND APPLICATION
www.elsevier.com/locate/ijmactool

On-line monitoring of depth of cut in AWJ cutting

Ashraf I. Hassan, C. Chen, R. Kovacevic *

Southern Methodist University, Department of Mechanical Engineering, Research Center for Advanced Manufacturing (RCAM), 1500 International Parkway, Suite 100, Richardson, TX 75081, USA

Received 23 September 2003; received in revised form 25 November 2003; accepted 3 December 2003

Abstract

Monitoring of the abrasive waterjet (AWJ) cutting process has become increasingly important. The present paper proposes a model for on-line depth of cut monitoring based on the acoustic emission (AE) response to the variation in AWJ depth of cut, instead of the expensive and impractical vertical cutting force monitoring. The main objective is to use the AE technique in order to predict the actual depth of cut in AWJ cutting under normal cutting conditions. It was found that the root mean square of the acoustic emission energy (AErms) increases linearly with an increase in the depth of cut and could be used for its on-line monitoring. The results show that the AE is the most suitable technique for AWJ monitoring, as the AE signal has high sensitivity to the variation in the depth of cut.

Keywords: Abrasive waterjet cutting; Vertical cutting force; Acoustic emission; Depth of cut

1. Introduction

Abrasive waterjet (AWJ) cutting has been the subject of much research work. Hashish [1,2] conducted a thorough theoretical modeling based on the mechanics of a single abrasive particle developed by Finnie [3] in the early 1960s. The main drawback of this model is its suitability for only ductile materials, whereas Zeng and Kim [4] developed an experimental model for ceramics.

From the little research work done so far, it was found that the vertical cutting force in AWJ varies due to the variation in the cutting parameters such as pressure, nozzle diameter, stand off distance, and flow rate. Table 1 summarizes the main studies carried out on the vertical cutting force in AWJ cutting. Kovacevic [7] found that the vertical cutting force increases with increasing pressure, abrasive flow rate and mixing tube diameter. Whereas, the vertical cutting force decreases with increasing stand off distance and it is only slightly affected by traverse rate. It was also found that a large increase in the magnitude of the vertical force indicates the presence of the mixing tube wear. This phenomenon could be utilized in monitoring of mixing tube wear. Another study [8] showed the importance of the ratio of the abrasive flow rate to water flow rate in affecting the vertical cutting force. However, monitoring the AWJ depth of cut using an on-line vertical cutting force measurement is expensive and impractical due to the erosive nature of the AWJ that affects the dynamometer components [5–7]. An alternative approach could be the use of the acoustic emission technique to monitor the depth of cut instead of using the vertical cutting force signal due to the ease of use of the AE technique and its low cost.

The acoustic emission (AE) technique has been applied to diverse fields of manufacturing processes because of its sensitivity to process parameters. Table 2 shows some of the applications of the AE technique to some of these processes. This technique has proved to be an effective means to monitor and control a wide range of diverse metal cutting processes [12]. Generally speaking, the AE technique could be applied to all machining processes involving friction, impact, plastic deformation, and fracture. Since the frequency content of the AE signal, typically in excess of 100 kHz, is well beyond the range of frequencies generally associated

* Corresponding author. Tel.: +1-214-768-4873; fax: +1-214-768-0812.
E-mail address: kovacevi@seas.smu.edu (R. Kovacevic).

0890-6955/$ - see front matter © 2003 Elsevier Ltd. All rights reserved.
doi:10.1016/j.ijmachtools.2003.12.002

Nomenclature

a	scale parameter
b	shift parameter
AErms	root mean square energy of the acoustic emission signal
C_1	constant representing the slope of the cutting force, depth of cut relation
C_2	constant representing the AErms at no load
C_3	constant representing the slope of AErms, depth of cut relation
d_n	waterjet nozzle, mm
d_m	mixing tube diameter, mm
F	vertical cutting force, N
h	depth of cut, mm
m_a	abrasive flow rate, g/s
P	waterjet pressure, MPa
S	stand off distance, mm
u	traverse rate, mm/min
α	normalization factor
$\psi(t)$	scaled wavelet functions

with the dynamic behavior of machine tools and cutting tools, the AE response is taken to be directly related to deformation, friction, and fracture mechanisms of the cutting process itself [13].

The fact that the workpiece material undergoes severe erosion under the action of the high-speed AWJ makes the AE technique ideal for the application of monitoring of the AWJ cutting process. It must be noted that the AE detects the waves generated by local deformation in a stressed material. Few attempts for the application of the acoustic emission technique to AWJ cutting were carried out in the past decade in order to monitor and control the process on-line. Table 3 reviews the main AE studies in the field of AWJ cutting. All of the studies used the frequency power spectrum that provides frequency information.

In this paper a signal processing method, known as the wavelet transform (WT), is introduced. The WT utilizes wavelets to perform a decomposition of the signal $x(t)$ into a weighted set of scaled wavelet functions $\psi(t)$. In general, for a function of $x(t)$ the wavelet transform energy can be defined by:

$$W_{a,b}^{x} = |\alpha|^{-1/2} \int_{-\infty}^{+\infty} x(t)\psi\left(\frac{t-b}{a}\right) \mathrm{d}t \tag{1}$$

in which α is a normalization factor, $\psi(t)$ is the mother wavelet with the scale parameter a (a, corresponds to a frequency band, Δ_a), and b is the shift parameter that provides a set of localized functions both in frequency and time. Unlike the Fourier transform that gives the precise frequency information, the wavelet transform provides band frequency information in the time domain. The band energy at the scale a can be computed by:

$$BE_{x}^{a} = \int_{-\infty}^{+\infty} \left| w_{a,b}^{x} \right|^{2} \mathrm{d}t \tag{2}$$

The characteristics of the wavelet transform make this method more suitable for the analysis of complex signals such as transient changes that are the symptoms of the sudden change of the processing state, which is the case in AWJ cutting. Unlike band pass filtering

Table 1
Cutting force studies for AWJ cutting

Application	Developed model	Experimental work	Authors
Analysis of energy transformation efficiency by vertical force measurements	Correlation between vertical force and energy transfer efficiency coefficient	Vertical force measurments for both WJ and AWJ	Momber 2001 [5]
On-line monitoring of surface roughness	Correlation between vertical force and surface roughness by curve fitting using ARMA modeling	Vertical force measurments for AWJ	Kovacevic et al. 1995 [6]
On-line monitoring of depth of cut	Correlation between vertical force and the depth of cut by curve fitting with step functions	Vertical force measurments at different cutting parameters for AWJ	Kovacevic 1992 [7]

Table 2
Acoustic emission models of selected manufacturing processes

Application	Phenomena	Experimental work and results	Authors
Friction stir welding	AE caused by friction and impact when the tool passes over a weld defect	Experiments on notched welded material;- graphs of band energy versus time and description of weld defects	Chen et al. 2003 [9]
Laser deburring	AErms varies with laser process parameters	Graphs of AErms versus distance, depth of cut and laser power	Lee Dornfeld 2001 [10]
Hard turning, grinding	AErms responds to the change in residual stresses	Graphs of AErms versus residual stresses and frequency	Tönshoff et al. 2000 [11]
Chip formation	AE responds differently to primary deformation zone, friction and wear	AE experiments of turning, drilling and grinding; graphs of AE energy versus time, flank wear and frequency	Dornfeld 1992 [12]
Micromachining (diamond turning)	AE is sensitive to very small chip thicknesses	Graphs of count rate and AErms	Liu Dornfeld 1992 [13]
Cutting tool wear	AE responds to the change in the worn cutting tool	Experiments of turning with different cutting speeds and feeds; graphs of AE count rate versus flank and crater wear	Teti 1989 [14]

Table 3
Acoustic emission models of AWJ

Application	Phenomena	Results	Authors
Monitoring of AWJ dissipated energy	AE energy increases with increase in AWJ dissipated energy	Time domain and frequency power spectrum; correlation between AErms and AWJ energy dissipation	Mohan et al. 2002 [15]
Monitoring of AWJ drilling depth of cut	AErms is reduced as drilling time, and hence depth of cut increase	Time domain and frequency power spectrum; correlation between AErms and depth of cut	Kovacevic et al. 1998 [16]; Kwak et al. 1996 [17]
Identification of different removal mechanisms	AE amplitude is sensitive to change in process parameters during cutting of concrete	Time domain and frequency power spectrum	Momber et al. 1995 [18]
Monitoring of AWJ depth of cut	AE amplitude has a high sensitivity to AWJ depth of cut	Time domain, frequency power spectrum and PSD vs. frequency	Mohan et al. 1994 [19]

where the bandwidth is constant, the band energy at each scale in the wavelet transform represents a different bandwidth. Wavelets at high frequency are of short duration, and wavelets at low frequency are of a relatively good frequency resolution. In theory, a specific frequency may correspond to a specific processing state. WT processing of the AE signals helps to extract features and to establish the relationship between the AE and the cutting parameters [9].

This paper presents a model for the response of the AE signal to the variation in the depth of cut. The main objective is to monitor AWJ cutting based on continuous measurements of the AE signal instead of the vertical cutting force signal.

2. Experimental work

A three-axis CNC abrasive waterjet machine is used in this work. The machine has the following specifications: work table movements: X-axis: 1219 mm, Y-axis: 1219 mm, and Z-axis movement: 200 mm. The high pressure intensifier has a maximum pressure rating of 60,000 psi (414 MPa) and power of 30 hp. A Paser 3™ abrasivejet cutting system is also used. The waterjet nozzle used throughout this work has an inside diameter of 0.33 mm, while the mixing tube has an inside diameter of 1.02 mm and length of 76 mm. Garnet as an abrasive material of Mesh No. 80 is used for all experiments. A strain gauge dynamometer is installed on the table of the AWJ machine that measures the vertical cutting force. The signal from the dynamo meter is transmitted to an amplifier and then to a data acquisition system at a sampling rate of 0.01 s. The force signal is analyzed by LabVIEW software. The AE energy with the corresponding data acquisition system is used to record the AE response of the AWJ at a 1 MHz sampling rate. The AE sensors are installed on the sides of the workpiece whose width is 13 mm. The recorded AE signals are preamplified with a gain of 20 dB. The set-up for the acoustic emission and the vertical cutting force measurements is shown in Fig. 1. Carbon steel AISI 1018 in the cold rolled con-

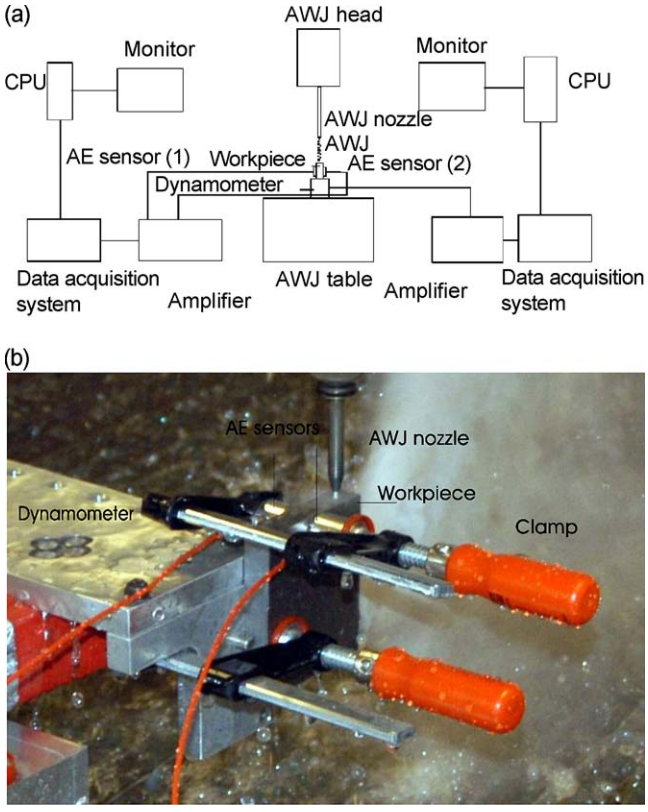

Fig. 1. AWJ acoustic emission and vertical cutting force measurements set-up. (a) Schematic of the set-up; (b) Close-up of the measurement set-up.

dition containing 0.15% C, is chosen as the workpiece material for the experiments. The dimensions of each sample are: 100 mm in length, 13 mm in width, and 65 mm in height. The vertical cutting force is measured for each sample from the beginning of the test up to a length of cut of 38 mm to ensure steady-state AWJ cutting conditions. Afterwards, each sample is machined by face milling to reveal the kerf surface, and three measurements of the depth of cut are taken in the steady state cutting zone and then averaged. However, the vertical cutting force signal is averaged and the AErms is calculated for only the steady-state cutting zone after excluding the entry zone. AWJ cutting conditions used in this study are listed in Table 4.

Table 4
AWJ cutting conditions

Parameter	Unit	Range
Waterjet pressure, P	MPa	100–350
Waterjet nozzle, d_n	mm	0.33
Traverse rate, u	mm/min	23
Abrasive flow rate, m_a	g/s	2.56
Stand off distance, S	mm	3
Abrasive mesh No	–	80
Mixing tube diameter, d_m	mm	1.02

3. Results and discussion

3.1. Vertical cutting force results

As the AWJ penetrates into the workpiece material, it is deflected in a direction opposite to the direction of the cutting head traverse, as in many other jet-like cutting processes such as laser and plasma beam cutting, forming the so-called "striation marks". The main force that is responsible for cutting is the vertical cutting force acting in the direction of the AWJ itself. Fig. 2 shows different vertical cutting force signals obtained at different pressures. AWJ starts to interact with the workpiece material, at B in Fig. 2a, causing a sudden rise in the value of the vertical cutting force. Afterwards, the vertical cutting force becomes stable from D to E in the stable cutting zone. The same trend of the vertical cutting force behavior with respect to time, for a pressure of 100 MPa, as shown in Fig. 2a, is also observed for all other pressures, as shown in Fig. 2b–d. However, the difference is that the magnitude of the vertical cutting force in the stable cutting zone increases as a result of the increase in pressure due to the increase in the abrasive particle velocity. It is apparent from Fig. 2 that the magnitude of force is small compared to that found in conventional metal cutting where the cutting force may reach up to 1000 N [20]. This result could be explained by the micro action of a large number of minute abrasive particles cutting successively in a localized kerf. The fact that the AWJ cuts the difficult to cut materials with small vertical cutting force is useful regarding the use of only simple and light fixtures for workpiece fixation on the machine table. Also, this result contributes to the achievement of a cold cutting process since the workpiece temperature may not exceed 70° [21,22].

Fig. 3 shows the effect of pressure on the depth of cut in AWJ. It is apparent from Fig. 3 that the depth of cut increases with an increase in pressure due to the increase of the particle velocity. Hence, abrasive particles impact the workpiece with a much higher velocity leading to an increased vertical cutting force. However, the response is not linear because the rate of increase in the depth of cut declines as the pressure increases.

The response of the vertical cutting force to the variation of the depth of cut is shown in Fig. 4. Fig. 4 clearly shows that the depth of penetration of AWJ in the material is reflected by an increase in the vertical cutting force. The experimental results, shown in Fig. 4, could be used to describe the linear relationship between the vertical cutting force (F) and the depth of cut (h) as:

$$F = C_1\, h \tag{3}$$

Eq. (3) provides a linear relationship between the achieved depth of cut in the AWJ cutting process and

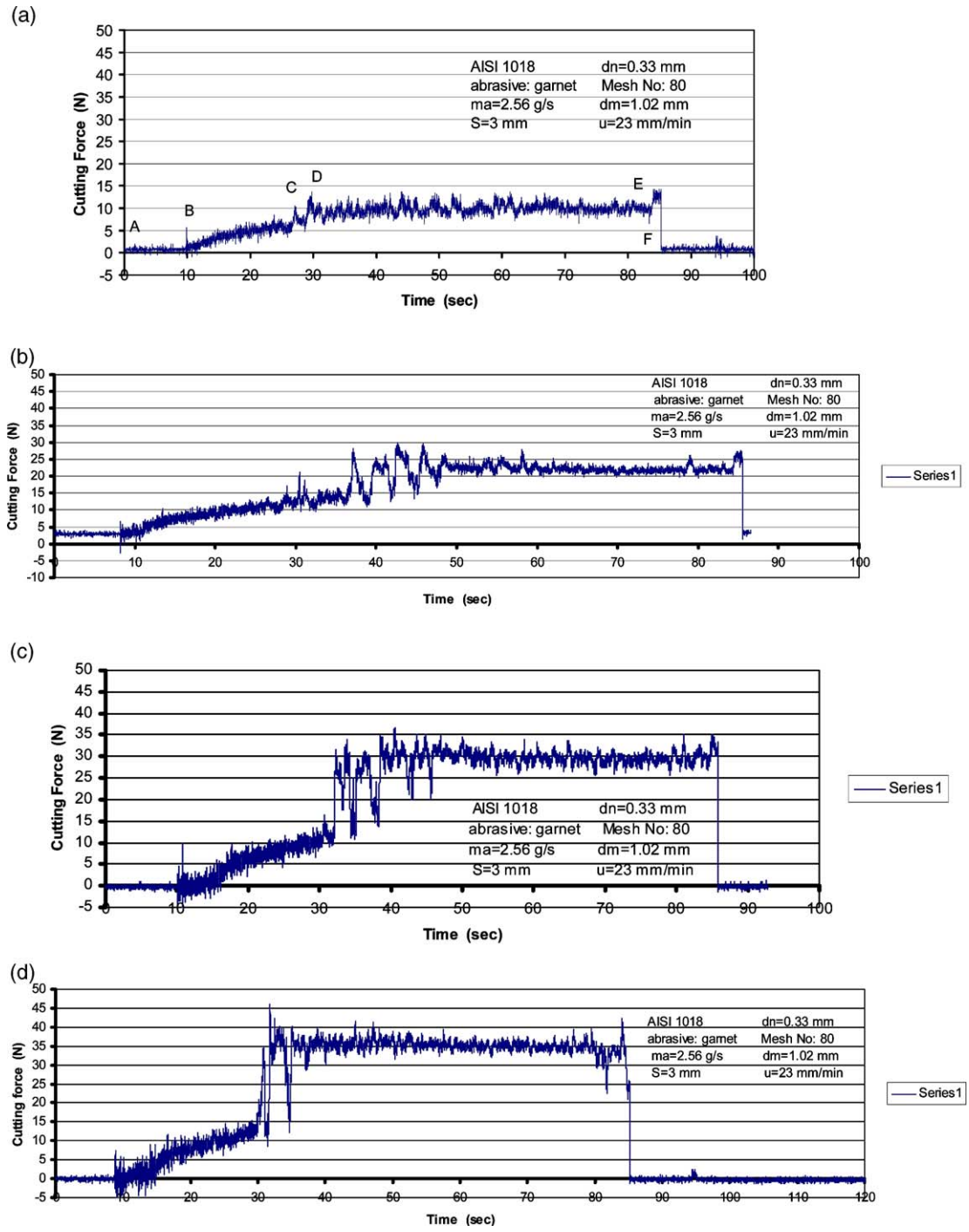

Fig. 2. AWJ vertical cutting force signal as a function of time at different pressures. (a) P=100MPa; (b) P=200 MPa; (c) P=300 MPa; (d) P=350 MPa.

the measured vertical cutting force. The depth of cut could be easily estimated from this equation by measuring the vertical cutting force during the actual cutting process. Moreover, it could be monitored on-line if the force signal is continuously recorded. For the current set of cutting conditions, the constant C_1 in Eq. (3) is equal to 0.6656.

3.2. AE monitoring results

Fig. 5 shows the variation of the acoustic emission band energy picked up by both sensors, as a function of time for a pressure of 100 MPa. Six scales of energy correspond to the following frequency band widths: (a) scale 1: 15.25, 31.25 kHz; (b) scale 2: 31.25, 62.5 kHz;

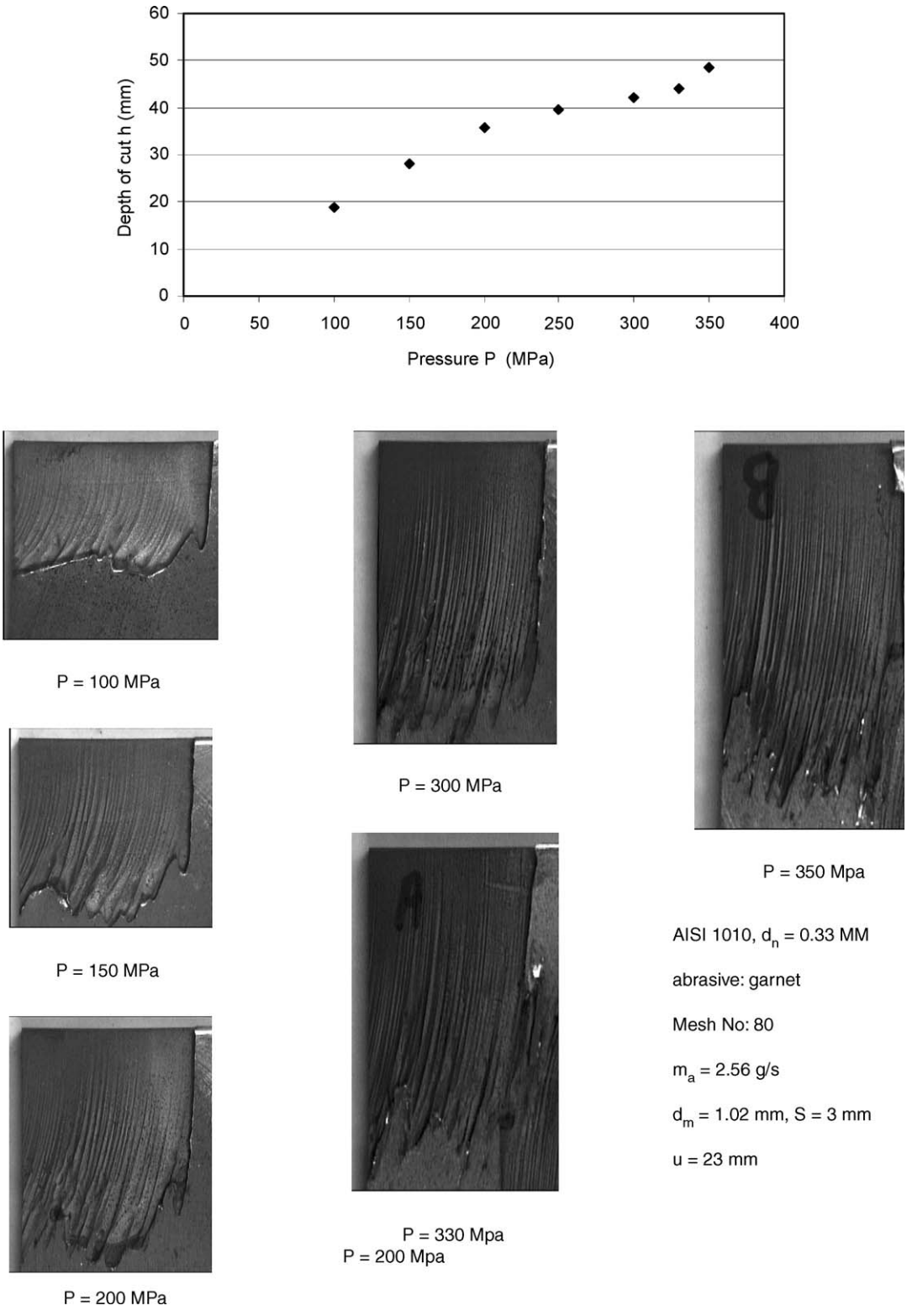

Fig. 3. Variation of the depth of cut with pressure.

(c) scale 3: 62.5, 125 kHz; (d) scale 4: 125, 250 kHz; (e) scale 5: 250, 500 kHz; (f) scale 6: 500, 1000 kHz [9]. Compared to the AE signals obtained from other manufacturing processes, the band energy of the AWJ cutting process is much higher in magnitude. As the jet impacts the workpiece surface at point (B), Fig. 5a, the level of the AE energy increases suddenly, while the impact of the jet with the workpiece material occurs.

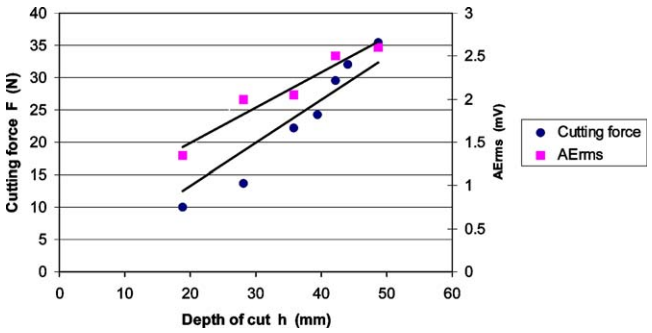

Fig. 4. Variation of the vertical cutting force and the AErms energy with depth of cut.

From B to C, Fig. 5a, the jet overcomes the entry zone, compared with the kerf in Fig. 5c. Beyond this zone up to D, the unstable acoustic emission response is characterized by a large variation of the AE energy. The significant increase in the AE band energy from B to D could be explained by the high dynamic interaction between the AWJ and the workpiece. Afterwards, the AE energy is suddenly reduced to zero due to the sudden shut down of the AWJ jet at E. Mohan et al. [19] found that the behavior of the AE signal with the depth of cut is the same even when the different depths of cut were obtained by changing pressure or traverse speed.

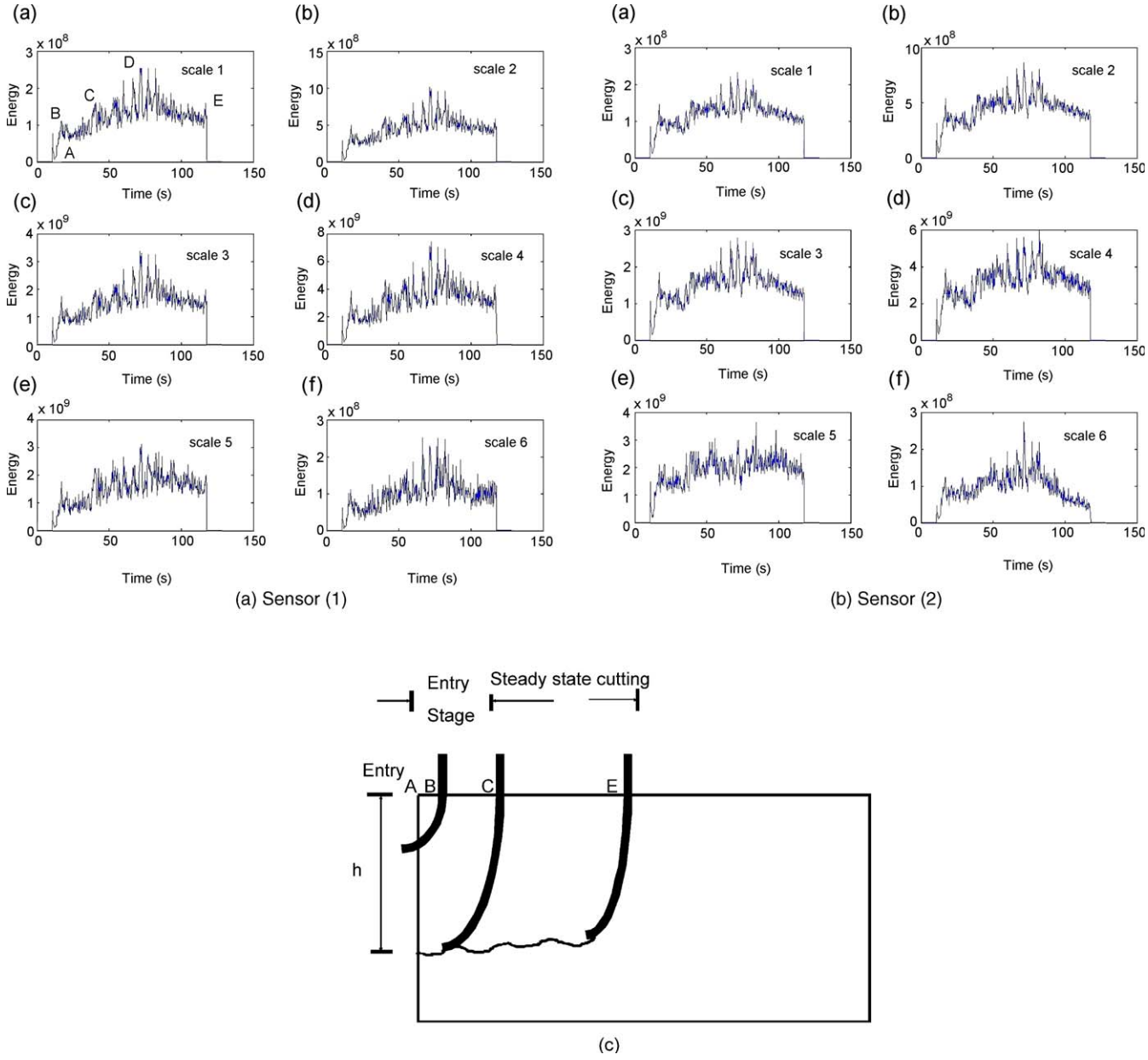

Fig. 5. Variation of the acoustic emission band energy with time at a pressure of 100 MPa. (a) Sensor (1); (b) sensor (2); (c) cutting zones of AWJ kerf.

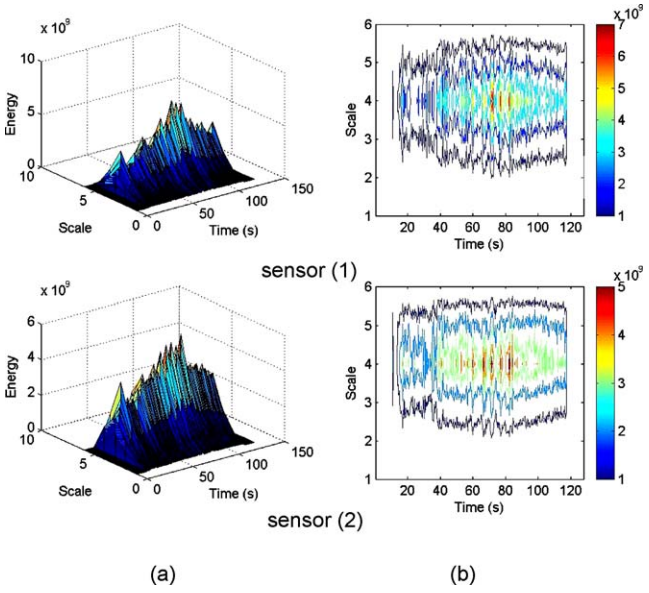

Fig. 6. Frequency power spectrum (a) and contour map (b) of acoustic emission band energy with time at a pressure of 100 MPa (same cutting conditions as shown in Fig. 5).

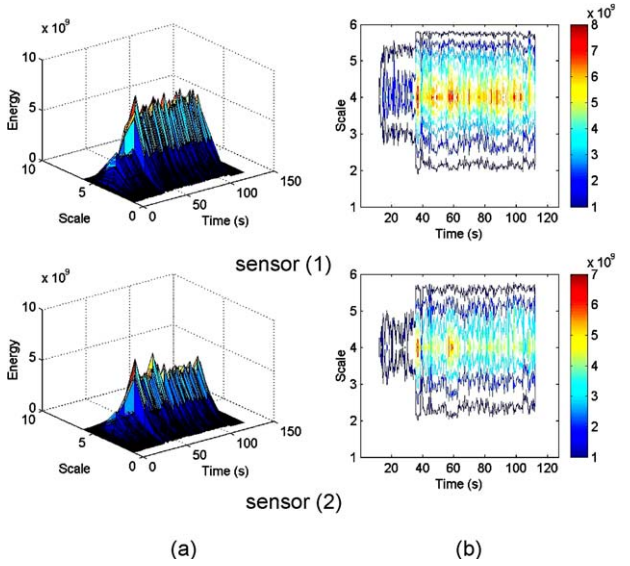

Fig. 8. frequency power spectrum (a) and contour map (b) of acoustic emission band energy with time at a pressure of 300 MPa (same cutting conditions as Fig. 7).

The frequency power spectrum and the contour map of the AE band energy are shown in Fig. 6. Fig. 6a shows the frequency power spectrum of the signal, which is a collection of band energies for a given set of the frequency scale and time. The peaks marking the start of the AWJ impact on the workpiece material and the deep penetration in the steady state cutting zone and the sudden shut down of the AWJ are clearly visible in the middle along the time axis. Fig. 6b shows the contour map which corresponds to the energy intensity at different points, displaying how the signal intensity of a different particular band frequency changes simultaneously with time. The dark spots in the middle of the map representing the higher energy levels, clearly indicate the high speed impact of the

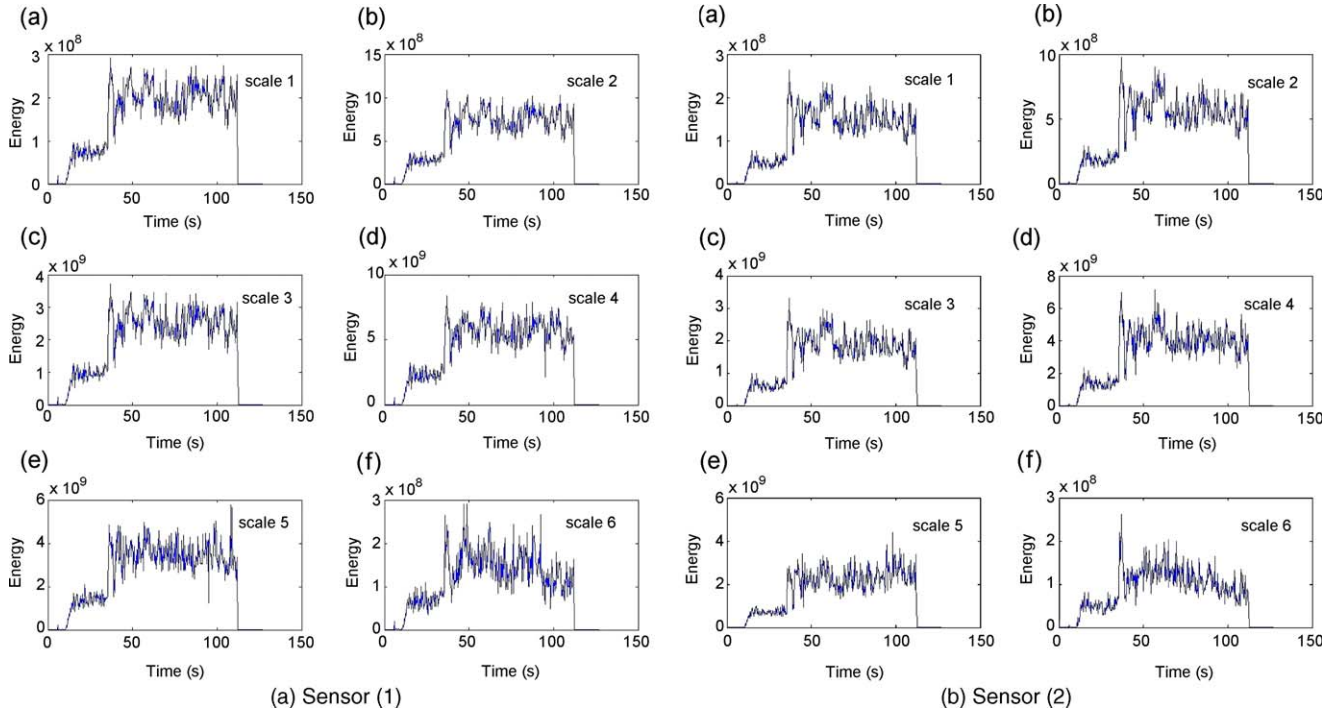

Fig. 7. Variation of the acoustic emission band energy with time at a pressure of 300 MPa.

AWJ with the workpiece material, and the steady state AWJ cutting after the removal of the initial entry cutting zone. It is also obvious that the main energy is in the frequency range of scale 1–4 with a peak at scale 4.

Fig. 7 shows the variation of the AE band energy with respect to time at a pressure of 300 MPa. The trend of the AE signal with respect to time for a WJ pressure of 100 MPa, as shown in Fig. 5, is also observed for the WJ pressure of 300 MPa. The main difference is that the magnitude of the AE energy increases as a result of the increase in the abrasive particle velocity due to the increase in the WJ pressure used. One of the useful methods to analyze the AE is to measure its energy content. The rate of energy released in the form of acoustic emission is usually evaluated by the root mean square (rms) voltage [11].

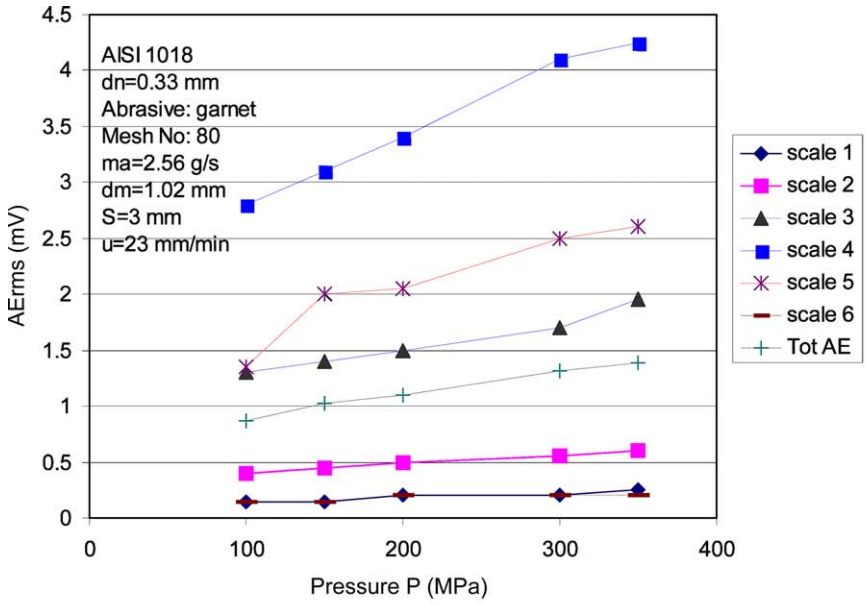

(a) Sensor (1)

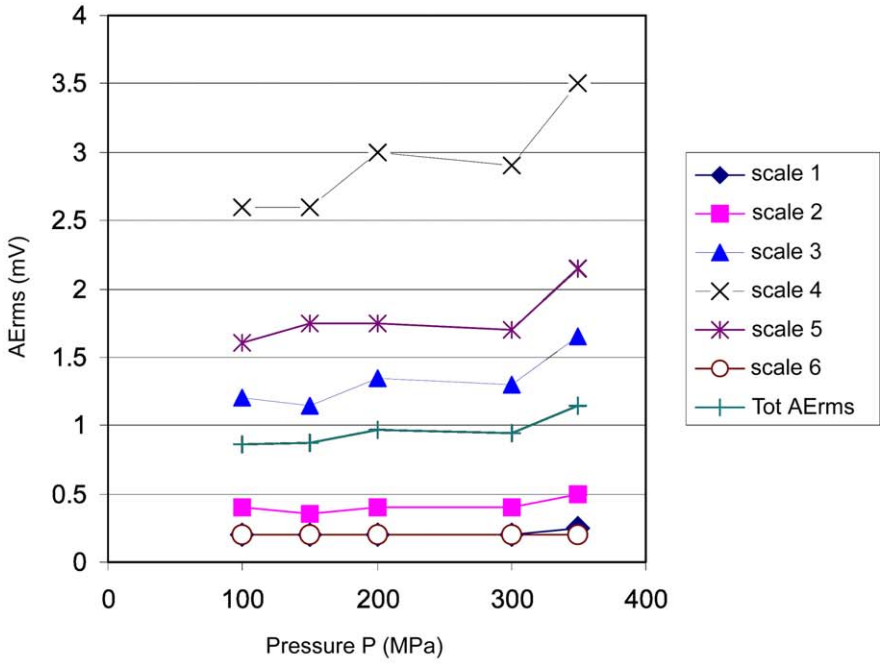

(b) Sensor (2)

Fig. 9. Effect of pressure on the AErms energy. (a) Sensor (1); (b) sensor (2).

The frequency power spectrum and the contour map of the AE band energy corresponding to a pressure of 300 MPa, are shown in Fig. 8. It is apparent from this figure that the energy level is much higher than its level for the pressure of 100 MPa, as shown in Fig. 6.

Fig. 9a shows the variation of the AErms energy of the signal with pressure for sensor (1). It must be noted that the calculation of the AErms energy of the signal is based only on the steady-state AWJ cutting. It is clear from this figure that for the total energy spectrum (Tot AErms) and the other spectra of low scales 1, 2, and 6, there is only a slight variation in the AE energy with pressure; whereas, at high frequency scales 3, 4 and 5, the AE energy increases with the increase in pressure. At scale 4, the acoustic energy experiences the maximum increase with the increase in pressure. The acoustic energy behaves the same way for sensor (2), Fig. 9b, but it has slightly smaller value of energy than sensor (1). It is apparent from Fig. 9 that the AErms at the scale of 4 could be taken as a means for monitoring the variation in pressure as it best represents the depth of cut, compared with the Tot AErms and the other AErms values at different scales.

The experimental results that describe the relationship between AErms (at scale of 4) and the depth of cut is shown in Fig. 4. It is apparent from this figure that the generation of the AE energy in AWJ cutting depends on the material removal rate or more precisely the depth of cut. Moreover, the AErms response to the variation in the depth of cut is more sensitive than the cutting force response, as shown in Fig. 4.

In terms of the root mean square of the acoustic energy (AErms), its relation with the depth of cut (h) can be linearly expressed as:

$$\text{AErms} = C_2 + C_3\ h \tag{4}$$

Eq. (4), which represents the energy consumption in AWJ cutting in terms of AErms energy, gives a theoretical basis for the prediction of the depth of cut in AWJ cutting. The depth of cut can be easily estimated from Eq. (4) by measuring the AErms level during the actual cutting process. In Eq. (4), the AWJ noise at no cutting accounts for the non-zero y-intercept. From the fitted line, the constants C_2 and C_3 in Eq. (4) could be determined. For the given experimental conditions, they are equal to 0.6752 and 0.0411, respectively.

From the previous analysis of the results of monitoring the depth of cut in AWJ cutting using both the vertical cutting force and the AE signals, it could be concluded that both techniques give a similar prediction of the depth of cut. However, monitoring the AWJ depth of cut using an on-line vertical cutting force measurement is expensive due to the high cost of the dynamometer and it is impractical due to the erosive nature of the AWJ which erodes the dynamometer components. Hence, an alternative approach could be the use of AE sensors to monitor the depth of cut instead of using the vertical cutting force signal due to the ease of use of the AE technique and its low cost. However, instead of the fixed AE sensors used in the current study, rolling AE sensors are recommended to be installed on the sides of the workpiece, while having the ability to translate with the cutting head to reflect the AE signal at the same location of the workpiece where the AWJ is cutting.

4. Conclusions

A model for on-line monitoring of the depth of cut in the abrasive waterjet cutting (AWJ) process, based on the acoustic emission (AE) response to the variation in the AWJ depth of cut was proposed instead of the expensive and impractical vertical cutting force measurement. As a result of the present model, the following conclusions could be drawn:

1. It was found that the AErms energy increases linearly with the increase in the depth of cut and could be used for its on-line monitoring instead of the vertical cutting force.
2. A model based on the response of the AErms signal to the variation in the depth of cut was developed and was used in its prediction.

Acknowledgements

The authors would like to express their gratitude to the Binational Fulbright Commission in Egypt for its research grant for the first author and the Research Center for Advanced Manufacturing, Southern Methodist University for its financial support of the present work. They are also grateful to Mr. Michael Vallant for his help in conducting the experiments.

References

[1] M. Hashish, A modeling study of metal cutting with abrasive waterjets, Trans. ASME, J. Eng. Mat. Technol. 106 (1) (1984) 88.
[2] M. Hashish, A model for abrasive-waterjet (AWJ) cutting, Trans. ASME, J. Eng. Mat. Technol. 111 (April) (1989) 154.
[3] I. Finnie, Erosion of surfaces by solid particles, Wear 3 (3) (1960) 87.
[4] J. Zeng, T.J. Kim, An erosion model of polycrystalline ceramics in abrasive waterjet cutting, Wear 193 (2) (1996) 207.
[5] A. Momber, Energy transfer during the mixing of air and solid particles into a high-speed waterjet: an impact force study, Exp. Therm. Fluid Sci. 25 (2001) 31.
[6] R. Kovacevic, R. Mohan, Y.M. Zhang, Cutting force dynamics as a tool for surface profile monitoring in abrasive waterjet, Trans. ASME, J. Eng. Ind. 307 (August) (1995) 340.
[7] R. Kovacevic, Monitoring the depth of abrasive waterjet penetration, Int. J. Mach. Tools Manufact. 32 (5) (1992) 725.

[8] W. König, A. Kämpfe, R. Mangler, M. Schmelzer, Einflüsse auf die Effecktivität des Wasserstrahlschneidens, DIMA 48 (7/8) (1994) 42.
[9] C. Chen, R. Kovacevic, D. Jandric, Wavelet transform analysis of acoustic emission in monitoring friction stir welding of 6061 aluminum, Int. J. Mach. Tools Manufact. 43 (13) (2003) 1383.
[10] S.H. Lee, D.A. Dornfeld, Precision laser deburring and acoustic emission feedback, Trans. ASME, J. Manufact. Sci. Eng. 123 (May) (2001) 356.
[11] H.K. Tönshoff, M. Jung, S. Männel, W. Rietz, Using acoustic emission signals for monitoring of production processes, Utrasonics 37 (2000) 681.
[12] D. Dornfeld, Application of acoustic emission techniques in manufacturing, NDT E Int. 25 (6) (1992) 260.
[13] J.J. Liu, D.A. Dornfeld, Monitoring of micromachining process using acoustic emission, Trans. NAMRI/SME XX (1992) 189.
[14] R. Teti, Tool wear monitoring through acoustic emission, Ann. CIRP. 38 (1) (1989) 99.
[15] R. Mohan, A. Momber, R. Kovacevic, Energy dissipation control in hydro-abrasive machining using quantitative acoustic emission, Int. J. Adv. Manufact. Technol. 20 (2002) 397.
[16] R. Kovacevic, H. Kwak, R. Mohan, Acoustic emission sensing as a tool for understanding the mechanisms of abrasive water jet drilling of difficult-to-machine materials, Proc. Inst. Mech. Eng. Part B: J. Eng. Manufact. 212 (1998) 45.
[17] H. Kwak, R. Kovacevic, R. Mohan, Monitoring of AWJ drilling of ceramics using AE sensing technique, Proceedings of the 13th International Conference of Jetting Technology, BHR Group, 1996, pp. 137.
[18] A. Momber, R. Kovacevic, R. Mohan, Acoustic emission measurements on brittle materials during abrasive waterjet cutting, Society of Manufacturing Engineers, Paper MR95-184, 1995.
[19] R. Mohan, A. Momber, R. Kovacevic, On-line monitoring of depth of cut of AWJ penetration using acoustic emission technique, in: N.G. Allen (Ed.), Water Jet Cutting Technology, Mechanical Engineering Publications Ltd, London, UK, 1994, pp. 649.
[20] C.A. Van Luttervelt, T.H.C. Childs, I.S. Jawahir, F. Klocke, K.V. Patri, Present situation and future trends in modeling of machining operations, CIRP. 47 (2) (1998) 587.
[21] R. Kovacevic, R. Mohan, H.E. Beardsley, Monitoring of thermal energy distribution in abrasive waterjet cutting using infrared thermography, Trans. ASME, J. Manufact. Sci. Eng. 118 (November) (1996) 555.
[22] M.M. Ohadi, A.I. Ansari, M. Hashish, Thermal energy distributions in the workpiece during cutting with an abrasive waterjet, Trans. ASME, J. Eng. Ind. 114 (February) (1992) 67.